Mobile robot navigation with a self-paced brain–computer interface based on high-frequency SSVEP

Pablo F. Diez, Vicente A. Mut, Eric Laciar and Enrique M. Avila Perona

Robotica / *FirstView* Article / November 2013, pp 1 - 15
DOI: 10.1017/S0263574713001021, Published online: 27 November 2013

Link to this article: http://journals.cambridge.org/abstract_S0263574713001021

How to cite this article:
Pablo F. Diez, Vicente A. Mut, Eric Laciar and Enrique M. Avila Perona Mobile robot navigation with a self-paced brain–computer interface based on high-frequency SSVEP. Robotica, Available on CJO 2013 doi:10.1017/S0263574713001021

Robotica: page 1 of 15. © Cambridge University Press 2013
doi:10.1017/S0263574713001021

Mobile robot navigation with a self-paced brain–computer interface based on high-frequency SSVEP

Pablo F. Diez†,‡,*, Vicente A. Mut‡, Eric Laciar† and Enrique M. Avila Perona‡

†*Gabinete de Tecnología Médica (GATEME), Facultad de Ingeniería, Universidad Nacional de San Juan (UNSJ), San Juan, Argentina*
‡*Instituto de Automática (INAUT), Facultad de Ingeniería, Universidad Nacional de San Juan (UNSJ), San Juan, Argentina*

(Accepted October 28, 2013)

SUMMARY
A brain–computer interface (BCI) is a system for commanding a device by means of brain signals without having to move any muscle. One kind of BCI is based on Steady-State Visual Evoked Potentials (SSVEP), which are evoked visual cortex responses elicited by a twinkling light source. Stimuli can produce visual fatigue; however, it has been well established that high-frequency SSVEP (>30 Hz) does not. In this paper, a mobile robot is remotely navigated into an office environment by means of an asynchronous high-frequency SSVEP-based BCI along with the image of a video camera. This BCI uses only three electroencephalographic channels and a simple processing signal method. The robot velocity control and the avoidance obstacle algorithms are also herein described. Seven volunteers were able to drive the mobile robot towards two different places. They had to evade desks and shelves, pass through a doorway and navigate in a corridor. The system was designed so as to allow the subject to move about without restrictions, since he/she had full robot movement's control. It was concluded that the developed system allows for remote mobile robot navigation in real indoor environments using brain signals. The proposed system is easy to use and does not require any special training. The user's visual fatigue is reduced because high-frequency stimulation is employed and, furthermore, the user gazes at the stimulus only when a command must be sent to the robot.

KEYWORDS: Brain–computer interface; Electroencephalography; Man–machine system; Mobile robot; Steady-state visual evoked potentials.

1. Introduction

A brain–computer interface (BCI) is a system that allows for commanding a device, such as a mobile robot, a speller or other systems, using only electroencephalographic (EEG) signals without moving any muscle. In the self-paced (asynchronous) mode, a BCI is constantly classifying the ongoing brain activity and is therefore always available for control.[1] That means, a BCI should be able to detect whether the user intentionally decides to perform specific mental tasks or, otherwise, does not generate any command (e.g. periods of thinking, daydreaming or reading).[2]

Different authors have proposed controlling a robotic device via BCI. For example, in 2004, Millan *et al.* proposed the control of a Khepera robot (5.7 cm diameter) using a BCI based on mental tasks and motor imagery classification.[3] Later on, a simulated mobile robot was driven using foot motor imagery in order to alternate between two modes: "no control" and "in control". The latter mode could steer the simulated robot using left- and right-hand imagery.[4] The P300 potential is an evoked response of the brain cortex elicited by an uncommon visual stimulus (e.g. oddball paradigm), which corresponds

* Corresponding author. E-mail: pdiez@gateme.unsj.edu.ar

to a negative potential that occurs 300 ms after the stimulus. P300 evoked potentials were obtained with a "stop/go" simulated car at stoplights in a virtual town.[5] In another report, a robotic vehicle was navigated through a maze using auditory P300.[6] A BCI was used by a quadriplegic subject to control a wheelchair on a virtual street populated with avatars.[7] Another BCI drove a simulated mobile system using the selection of stable user-specific EEG features that maximized the ability to separate different mental tasks.[8] Later on, that BCI was applied to drive a wheelchair.[9] A fuzzy shared-control also was proposed for an assistive navigation architecture based on sparse and discrete human–machine interface.[10] Similar P300/BCI designing philosophies were tested in a HOAP2 humanoid robot with a bit rate of up to 24 bits/min with an accuracy of 95% over four choices.[11] The same humanoid robot learned some movements (such as walking, grasping) through self-paced mental imagery BCI and, thereafter, the user could send high-level commands using P300 so that the robot repeated the learned movements.[12] A mobile robot was controlled using four commands derived from two mental tasks (i.e. relaxed state and right-hand imagination).[13] The robotic group directed by Minguez developed several BCI for controlling robotic systems. For instance, a wheelchair was commanded using P300 evoked potentials,[14] and later on a teleoperated mobile robot was manoeuvred by a BCI.[15] The same group reported also a telepresence system.[16]

All of these projects made use of mental tasks, motor imagery or P300 for controlling the robotic systems.[3–16] However, such systems generally require a training step that can necessitate from some minutes up to hours or even days. In addition, the user is sometimes subject to mental efforts that could produce mental fatigue.

Another paradigm applied in BCI is Steady-State Visual Evoked Potentials (SSVEP), which can be used by most candidates with relatively no training. It tends to outperform other BCIs in terms of information transfer rates. A SSVEP is a resonance phenomenon arising mainly in the visual cortex when a person is gazing at a flickering light with a frequency above 4 Hz[17] and can be elicited up to at least 90 Hz.[18] This range could be divided into three sub-ranges: low- (up to 12 Hz), medium- (12–30 Hz) and high-frequency (>30 Hz).[17] The SSVEP in low-frequency range has higher amplitude responses than in the medium range. Consequently, the larger the amplitude of the SSVEP, the easier its detection. The weakest SSVEP is found on the high-frequency range. However, spontaneous EEG (considered here as noise) decreases on higher frequency bands, hence, the signal to noise ratio is similar on the three ranges.[19] High-frequency SSVEP has the advantage of a great decrease of visual fatigue caused by flickering,[20–22] making the SSVEP-based BCI a more comfortable system.[22] Moreover, low- and medium-frequency SSVEP ranges interfere with alpha rhythm, and could cause an epileptic seizure as well.[23] Despite that, SSVEP-based BCI are mainly focused on the low- and medium-frequency range. Specifically, SSVEP-based BCIs controlling a mobile robotic system use low,[24] medium[25] or both frequency ranges.[26] In 2008, a robotic prosthesis was controlled with SSVEP[27] and recently, a controlled robotic assistant for grasping objects was commanded using stimulation in the medium frequency range.[28] However, navigating a robotic mobile system with the help of a SSVEP-based BCI is a recently developed area in the BCI community.[25]

The work by Mandel and colleagues reports that eight out of nine untrained subjects successfully navigated an automated wheelchair using SSVEP, ranging from 13 up to 16 Hz, and requiring merely 10 min of preparation.[25] A Light-Emitting Diode (LED) stimulation box flickering at 10, 11, 12 and 13 Hz was used to move a small robot employing two different approaches: one using minimum energy and another using Fast Fourier Transform and Linear Discriminate Analysis.[26] Recently, in 2010, a robotic mobile system was commanded by a SSVEP-based BCI using 5 up to 6.9 Hz with a statistical test for feature extraction (Spectral *F*-test) and classification performed by a rule-based classifier.[24] An algorithm for asynchronous BCI control using high-frequency SSVEP was recently developed by our research group, where six subjects could control a mobile object on the screen through different scenarios, reaching up to 45 bits/min.[29] Perhaps, the first time a robot was controlled with high-frequency SSVEP was presented by Volosyak and colleagues.[30] In that research, a tiny robot was moved in a maze through fixed positions with stimuli of 34, 36, 38 and 40 Hz, reaching an average speed of 12.10 bit/min and an average accuracy of 89.16%.

The aim of this study was to develop a complete strategy to control a mobile robot using an asynchronous high-frequency SSVEP-based BCI. The experiments were performed within a real office environment. Since the user and the robot were in different locations, the robot was remote-commanded through a video image showing the path to the subject. The BCI commanded the robot together with an algorithm to avoid obstacles, thus allowing for comfortable and safe navigation.

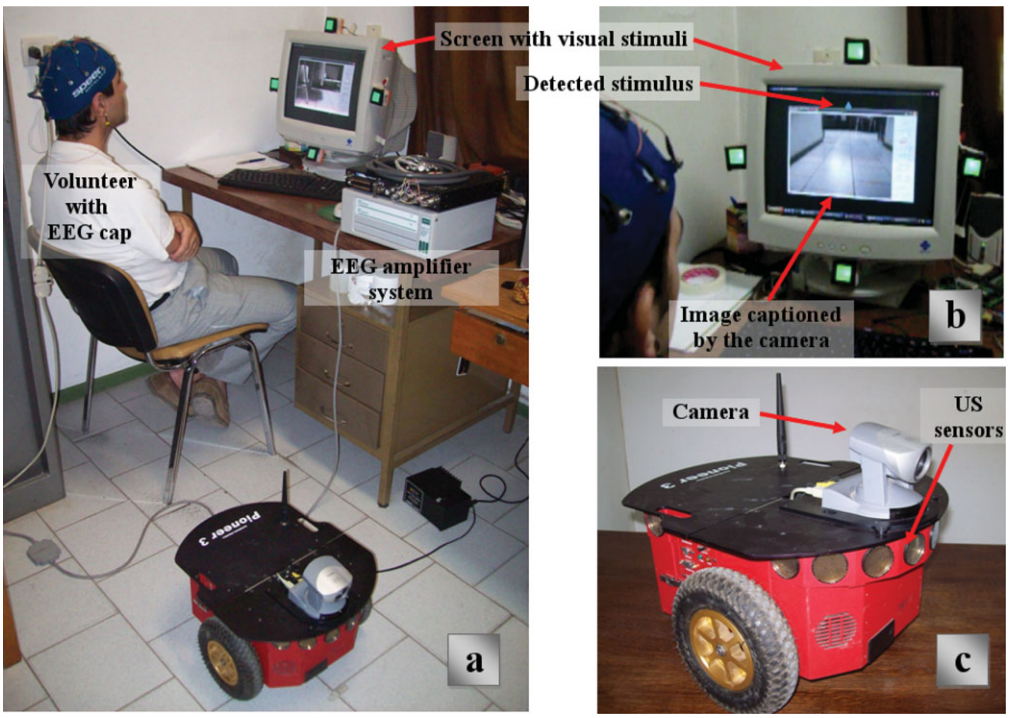

Fig. 1. (Colour online) (a) A volunteer sat in front of a PC screen rounded by four flickering stimuli, EEG amplifier system and robot. (b) The interface screen with the video image captioned by the robot and the blue arrow is indicating the detected stimulus (top in this case). (c) Robot Pioneer 3-DX with Canon VC-C4 camera and ultrasonic sensors.

In the next section, the problem is described and the experimental conditions are established. In Section 3, the EEG signal processing method, the robot control algorithm and finally, the interconnection between these two parts are explained. In Section 4, the results are reported. Then, these results are discussed in Section 5, and the final section presents the conclusions.

2. Problem Definition

In this section, the objective of the research, the equipment and experimental conditions are described. In the proposed experiment a BCI was used to remotely command a mobile robot, which is navigated towards a determined position in a real office-like environment. Seven volunteers, who previously agreed to participate in the experiment, sat in a comfortable chair looking at a monitor with four stimulating boxes on each side. The boxes (2.5 cm $\times$ 2.5 cm) were illuminated by high efficiency LEDs (Figs. 1a and 1b). The flickering frequencies were almost imperceptible to the user, because LEDs kindled at 37 (top), 38 (right), 39 (down) and 40 Hz (left), respectively. Each frequency was precisely controlled by an FPGA Xilinx Spartan2E, programmed by the computer. The flickering frequencies could be modified by simple reprogramming.

The EEG was acquired with three channels over the visual cortex at positions O_1, O_z and O_2, referenced to F_Z and grounded at linked A_1-A_2. EEG signals were amplified with a Grass 15LT system, pass-band filtered between 1 and 100 Hz and with a notch filter for 50 Hz line interference. Then, the EEG was digitalized with a NI-DAQPad6015 at a 256 Hz sampling frequency with 16-bits resolution for each channel (Fig. 1a).

A robot Pioneer 3-DX (45$\times$ 38$\times$ 23 cm) was used in the experiments with a Canon VC-C4 camera mounted on it (Fig. 1c). The volunteers watched on the screen the images of the path along which they drove the robot (Fig. 1b). Communication between robot and computer was wireless (standard Wi-Fi). Sixteen ultrasonic (US) sensors placed around the robot were used to detect obstacles. A scheme of the experimental setup is depicted in Fig. 2.

When the user wanted to convey a command to the robot, he/she gazed at a certain stimulus, and then the BCI detected the user's intention. Therefore, the BCI could produce four commands to the robot, i.e. "advance", "turn right", "turn left" and "stop", each corresponding to top, right, left and

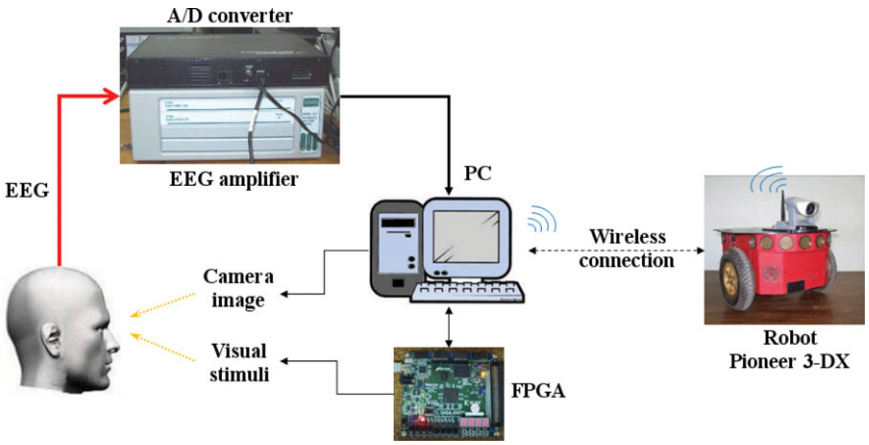

Fig. 2. (Colour online) Scheme of the experimental setup.

down visual stimulus, respectively. Then, the robot moved to the desired direction, and since the environment was changing around the robot, the new situation was captured by the camera. Finally, the user observed those changes on the screen and decided to send a new command. The robot advanced at constant velocity of 100 mm/s while the angular velocity was limited to 0.653 rad/s (37.4 deg/s). These velocities were restricted for safety reasons, because the algorithm was designed for a future extension to command a wheelchair.

3. Methods

This section presents the EEG signal-processing method, the robot control algorithm and finally, the interconnection between these two parts.

3.1. EEG signal processing

The EEG signals were processed with a method described in the bibliography.[29] First, the signal was digitally filtered with a 6th-order Butterworth band-pass filter, with cut-off frequencies set at 32 and 45 Hz. Then, the power spectral density was estimated using the periodogram $\hat{S}(f)$, as follows,

$$\hat{S}(f) = \frac{T_s}{N}\left|\sum_{n=0}^{N-1} x[n]e^{-j2\pi f n T_s}\right|^2 \tag{1}$$

where T_S is the sampling period, N stands for the number of samples and f represents the frequency. To compute the periodogram, the Fast Fourier Transform (FFT) with 2s-long rectangular window was used. The window was moved in 0.25 s steps. Figure 3 depicts the periodogram of four different EEG segments, where the SSVEP peaks elicited by each stimulating frequency can be observed. After that, the normalized power $P(f_i)$ at each stimulation frequency f_i ($i = 37$, 38, 39 or 40 Hz) was computed by,

$$P(f_i) = \sum_{ch=1}^{M} \frac{\hat{S}_{ch}(f_{i\mp}0.25)}{\widehat{BL}_{ch}(f_{i\mp}0.25)}/M \tag{2}$$

where ch is the number of channels from 1 to $M = 3$(O_1, O_z and O_2 channels were used); BL_{ch} is the periodogram of the baseline EEG. For each volunteer, a baseline EEG was acquired in advance to the experiment. They were asked to get focused on a point at the centre of the screen for 60 s, but without focusing on any stimuli (which were flickering). This baseline was used for equalization of the EEG spectrum[29] due to the low power EEG spectrum of higher frequencies. For example, an SSVEP at 38 Hz has greater power than another SSVEP at 40 Hz.[29] This calculation was performed every 0.25 s, and an SSVEP was labelled as one of the four possible classes (top, right, bottom or left) according to:

$$class(f_i) \Leftarrow \max\left\{P(f_i)_{(n)}\right\} = \max\left\{P(f_i)_{(n-1)}\right\} = \ldots = \max\left\{P(f_i)_{(n-10)}\right\} \tag{3}$$

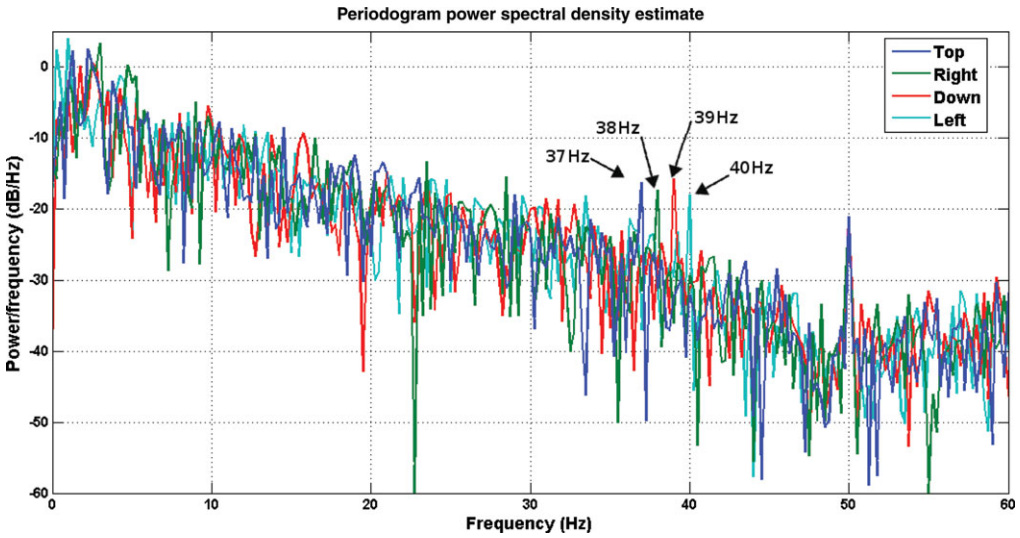

Fig. 3. (Colour online) Power spectral density of four different EEG segments, each one corresponding to a different stimulus (top, right, down and left). Then, the four peaks are mapped into the four commands sent to the robot (advance, turn right, stop and turn left).

Therefore, when the maximum $P(f_i)$ corresponding to the same f_i is maintained for at least 10 consecutive samples (i.e. 2.5 s), the SSVEP corresponding to f_i is detected and the EEG segment is labelled as the *class*(f_i). Finally, whenever this condition is not satisfied, the EEG segment is classified as belonging to an undefined class.

Online feedback was presented to the user indicating the detected stimulus. This was performed in two simultaneous ways: a visual feedback, which consisted of a blue arrow on the screen (see Fig. 1b), and an audible feedback, which consisted of a voice that names the detected stimulus (i.e. "right", "left", "forward" or "stop", in Spanish).

3.2. Robot control algorithm

The control algorithm used for moving the robot was proposed by a co-author of this research.[31–32] Consider the unicycle-like vehicle is initially positioned at any non-zero distance from the target position p_2 (Fig. 4a). The robot motion towards p_2 is governed by the combined action of both, the angular velocity ω and the linear velocity u, describing the vehicle position in polar coordinates and considering the distance error e calculated from the actual position p_1 and the desired position p_2. Besides, the orientation error α was defined according to the actual orientation of the robot φ and the desired orientation θ as $\alpha = \theta - \varphi$. Then, the kinematic equations were defined as,

$$\begin{cases} \dot{e} = -u\cos\alpha \\ \dot{\alpha} = -\omega + u\frac{\sin\alpha}{e} \\ \dot{\theta} = u\frac{\sin\alpha}{e} \end{cases} \tag{4}$$

The chosen state variables are e and α, and assumed as directly measurable for any $e > 0$. Let us consider the Lyapunov-like candidate function,

$$V_{(e,\alpha)} = \frac{1}{2}\lambda e^2 + \frac{1}{2}\alpha^2 \quad \text{with} \quad \lambda > 0 \tag{5}$$

Its time derivative $\dot{V}$ along the trajectory described in Eq. (4) is given by,

$$\dot{V} = \lambda e\dot{e} + \alpha\dot{\alpha} = \lambda e\,(-u\cos\alpha) + \alpha\left(-\omega + u\frac{\sin\alpha}{e}\right) = \dot{V}_1 + \dot{V}_2 \tag{6}$$

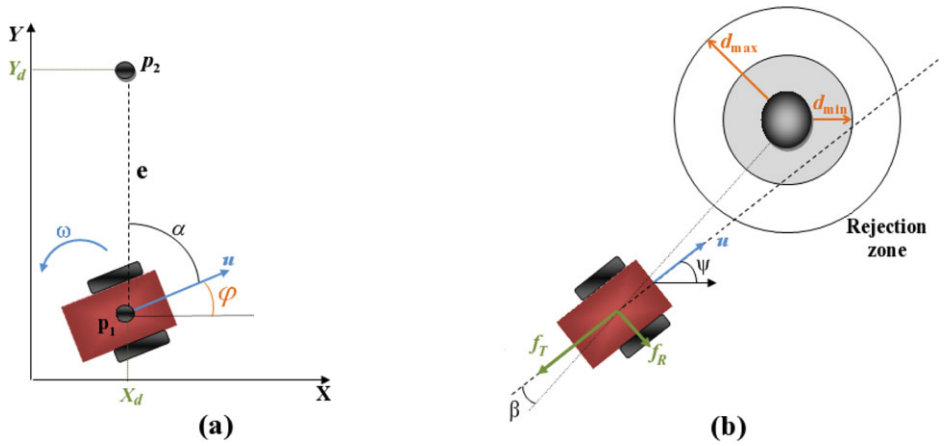

Fig. 4. (Colour online) (a) Robot in p_1 and its final destination (p_2). (b) Robot evading an obstacle.
Note: u is velocity of the robot; e is the error distance between the actual position (p_1) and the desired position (p_2); α is the error on the orientation of the robot; f_R is the radial and f_T is the tangential fictitious force; β is angle of interaction with obstacle; ψ is the rotation angle to avoid obstacle.

The first term in Eq. (6), corresponding to $\dot{V}_1$, can be non-positive by letting the linear velocity u have the smooth form,

$$u = \gamma \tanh e \cos\alpha \quad \text{with} \quad \gamma = |u_{max}| \tag{7}$$

where $u_{\max}$ is the maximum velocity of the robot. The hyperbolic tangent term is used to avoid actuator saturation. Then, considering Eq. (7) in the second term of Eq. (6), $\dot{V}_2$ can also be non-positive by letting the angular velocity have the smooth form,

$$\omega = k_1\alpha + \lambda\frac{\tanh e}{e}\sin\alpha\cos\alpha \tag{8}$$

where k_1 is the controller gain and $|\omega_{max}| = k_1\pi + 0.5\gamma$, and thus leading to the following expression for the time derivative of the original Lyapunov function V,

$$\dot{V} = -\lambda\gamma e \quad \tanh e\cos^2\alpha - k_1\alpha^2 \; < \; 0 \tag{9}$$

The latter equation results in a negative definite function. That means asymptotic convergence to zero of the state variables, thus verifying the control objective, i.e.

$$\begin{cases} e_{(t)} \\ \alpha_{(t)} \end{cases} \rightarrow 0 \quad \text{when } t \rightarrow \infty \tag{10}$$

Here, k_1 was set as 0.4 and the desired orientation φ could take the following values: $\pm\,\pi/2$ rad for turns or 0 rad to move forward. This is due to the actions required for moving in an office-like environment (a house or a maze), typically similar to the one tested. However, the robot can depart from these routes when trying to avoid an obstacle. Thereafter, the desired position p_2 is calculated away from p_1. The new coordinates (X_d, Y_d) on the reference system indicating the desired position p_2 are calculated as $X_d = X + \mathrm{k}_2\cos\alpha$ and $Y_d = Y + \mathrm{k}_2\sin\alpha$ (k_2 is a constant empirically estimated as 10).

To skip obstacles, the robot velocities u and ω had to be modified. This was performed using the impedance (Z) concept, for which the mechanical interaction was substituted for a distance and a non-contact interaction by taking into account the distance from the robot to the detected obstacle.[33] Hence, a fictitious force was generated when an obstacle was detected, moving the robot out of the rejection zone (Fig. 4b), defined as,[34]

$$f_{(t)} = a - b\left(d_{(t)} - d_{\min}\right) \tag{11}$$

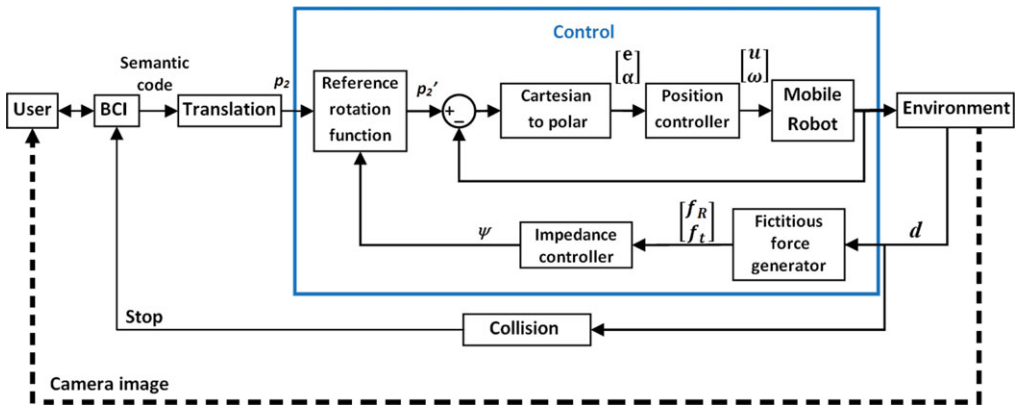

Fig. 5. (Colour online) Scheme of control loops and BCI-robot interaction.

where a and b are positive constants, so that $a - b(d_{\max} - d_{\min}) = 0$; $d_{\max}$ is the maximum robot-obstacle distance; $d_{\min}$ is the minimum robot-obstacle distance and $d_{(t)}$ is the actual robot-obstacle distance. In this experiment, $d_{\max}$ is 40 cm and $d_{\min}$ is 25 cm. These values were chosen because one of the objectives of this research was to allow navigating the robot within real environments, that is, where short distances (<100 cm) separate the obstacles in the environment.

The fictitious force f was decomposed into its orthogonal components, namely, the radial (f_R) and tangential (f_T) components, depending on the angle β. After that, the impedance Z was calculated as,[35]

$$Z = Bp + K \tag{12}$$

where p stands for the derivate operator, constant B represents a damping effect and K is a spring effect arising from the virtual interaction between the mobile robot and the obstacle. In this work, B and K were empirically determined as 0 and 0.2, respectively.

The rotation angle ψ to avoid the obstacle with respect to the vehicle centre was computed as,

$$\psi = Z^{-1} f_T \operatorname{sign}(f_R) \tag{13}$$

Finally, a rotation transformation was used to obtain the new desired position p_2', as,

$$p_2{}' = \begin{bmatrix} \cos\psi & -\sin\psi \\ \sin\psi & \cos\psi \end{bmatrix} p_2 \tag{14}$$

In Eq. (14) the desired location p_2 was modified and then, velocities u and ω recalculated to avoid an obstacle.

3.3. Interaction BCI-Robot

In order to attain comfortable navigation of the robot, the interaction between the BCI commands and the robot movements must be considered. Figure 5 shows a scheme of control loops on the proposed system. When the user wants to convey a command (advance, turn left, turn right or stop) to the robot, he/she must gaze at a stimulus, then the BCI must detect the user intention and generate a semantic code. This semantic code must be translated into the position of the newly desired location p_2. Finally, the control signals u and ω are generated as depicted in Eqs. (7) and (8). Then, the robot moves on the desired direction. Consequently, the environment around the robot changes and these changes are captured by the camera. Finally, the user closes this outer loop by making a new decision (or not).

When an obstacle is detected within the trajectory of the robot by US sensors, the avoidance obstacle algorithm modifies both u and ω in order to evade the obstacle. This is performed by the inner control loop. On the other hand, in some cases the robot cannot avoid the obstacle; for example, if the obstacle is right in front of the robot (e.g. a wall) or may be a possible collision (i.e. the obstacle

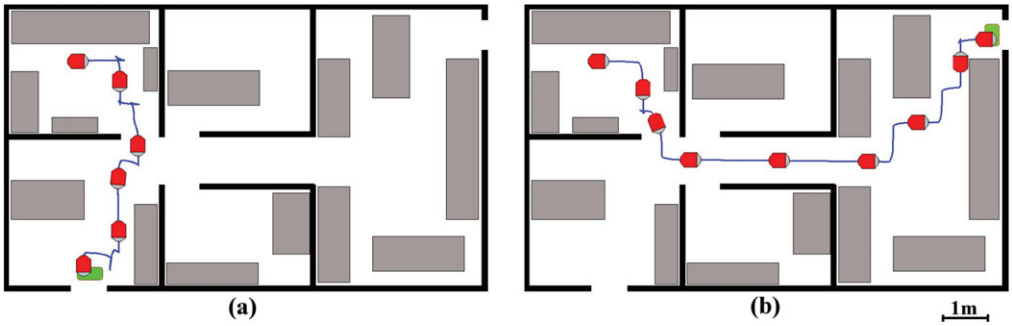

Fig. 6. (Colour online) The robot path through the office environment towards two different places. The grey figures represent the desks and shelves. The green figures illustrate the two possible destinations. (a) Destination 1, Volunteer 5 navigating towards the first (easier) place; (b) Destination 2, Volunteer 2 navigating towards the second place.

is at less than $d_{\min} = 25$ cm). Then, the robot stops and prompts the user for a new decision. Note that the robot moves back 10 cm before stopping in order to perform the next command successfully.

In this approach, the user does not need to gaze constantly at a stimulus to move the robot, because the robot moves forward along the selected direction until a new command is received (e.g. a different direction or a stop command). In other strategies,[26] when the subject was not looking at the stimuli, the robot was stopped. Our approach represents an advantage because the user could look at other things instead of the stimuli, such as the camera image (in this particular case) or the surrounding environment (in a wheelchair) or simply nothing in particular and remain relaxed.

4. Experimental Results

Seven healthy volunteers (six men, one woman, aged 25.9 ± 4.8 yrs) participated in the experiment, they had no previous experience in BCI or robotics (except volunteers 1 and 6, who had participated in a previous BCI experiment). They were asked to navigate the robot towards two different places in a real office environment, with many shelves and desks. The first place is easier to reach than the second one (Fig. 6). Thus, the volunteers intended to reach the first (easier) place (Fig. 6a) until they attained optimal performance (i.e. they felt as if they could control the robot). Later, they intended to reach the second place (Fig. 6b), as many times as they wanted. In this sense, each subject performs a different number of trials depending on his own performance. These two places were named *Destination 1* and *Destination 2*, respectively. Destination 1 and 2 are two access doors to the environment; hence the task of the volunteers was to navigate the robot to those doorways.

In Fig. 7a the SSVEP calculated for the four stimuli according to Eq. (2) is shown. Besides, the commands sent by the BCI to the robot are presented in Fig. 7b, where the red line indicates the commands forward, right, left or stop and, blue circles represent each time a SSVEP is labelled as one class (according to Eq. (3)) and a command was sent to the robot. Sometimes these commands were redundant, i.e. the same command is detected twice or even more. This is due to the volunteers who keep gazing at the stimulus for a few more seconds. These redundant commands are ignored by the system and they were not conveyed to the robot. For example, at 16 s the right stimulus power became the maximal power (green line in Fig. 7a) and 2.5 s later, at 18.5 s the command right is conveyed to the robot (Fig. 7b). Therefore, the robot turned to the right and went in that direction. At 21 s a redundant command was ignored and was not conveyed to the robot. Later, at 33 s the left stimulus is detected and the robot turned to the left. When red line in Fig. 7b indicates a "0" state (during 41–62 s, 115–121 s or 133–137 s), the robot was stopped by the control algorithm to avoid a collision. This situation is communicated to the user (audible feedback) and the system will wait for a new command. SSVEP and commands depicted in Fig. 7 were extracted when Volunteer 5 navigates the robot towards Destination 1 (Fig. 6a).

Table I illustrates the performance parameters attained by each volunteer for Destination 1. This table shows the elapsed time in each trial and the number of commands sent to the robot. Since the path to reach Destination 1 is pre-established, the commands could be classified as correct or wrong; i.e. when a command deviates the robot from this path, then it is a wrong command. For example, in

Table I. Results for Destination 1.

		Commands			
Volunteer	Trial	Time (s)	Wrong	Correct	Stop by control system
1	1	130	0	17	2
2	1	150	0	20	1
3	1	228	1	23	5
4	1	205	4	17	2
5	1	164	2	14	3
6	1	210	6	25	3
7	1	220	2	10	1
	2	150	2	9	2
Average		182.13	2.13	16.88	2.38
Std. Dev.		37.70	2.03	5.74	1.30

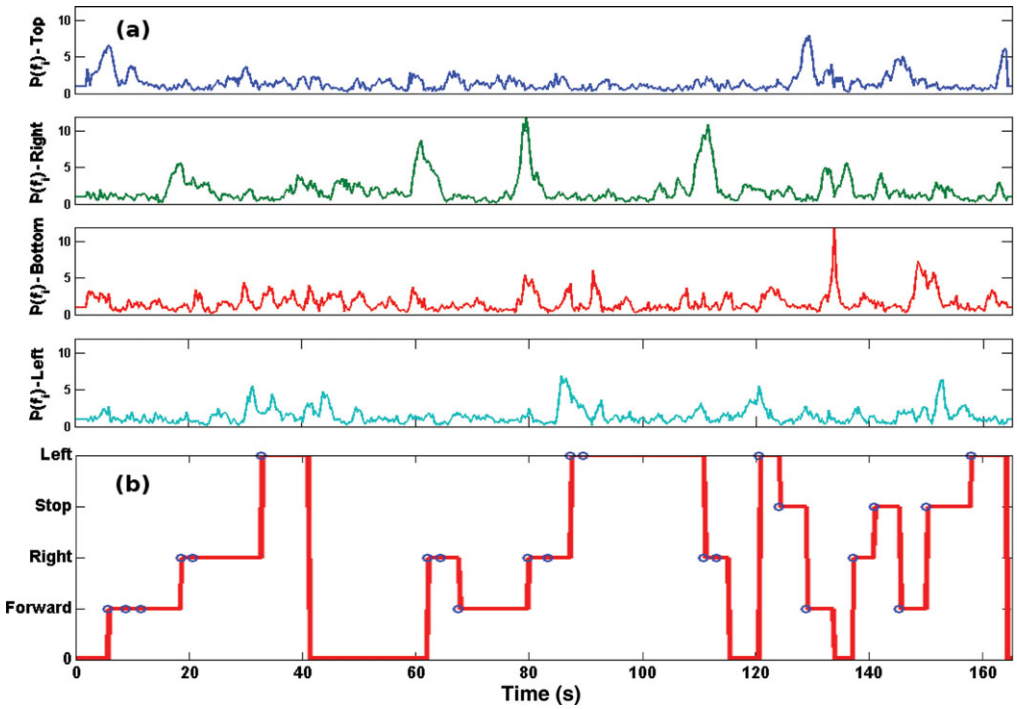

Fig. 7. (Colour online) (a) Power of the SSVEP calculated for each stimulus (top, right, bottom and left); (b) Commands sent by the BCI to the robot (advance, turn right, stop and turn left). These values were calculated online when Volunteer 5 navigated the robot towards Destination 1.

Destination 1, when the robot goes through the doorway of the first room it should turn to the right, then a left command is considered wrong. However, the user could wish to stop the robot with down stimulus and this was not considered a wrong command. Table I also presented the number of times that control algorithm stops the robot in order to avoid a collision, i.e. an obstacle is too close. For example, Volunteer 5 has three stops and they are depicted as "0" state in Fig. 7b. Volunteers attained optimal performance in the first trial, except Volunteer 7, who required two trials. Then, volunteers performed the next task, Destination 2. In Table II the same results are presented but evaluated for Destination 2.

Finally, in Fig. 8 linear and angular velocities of the robot, when commanded by Volunteer 5 towards Destination 1 (corresponding with situation depicted in Figs. 6a and 7), are presented. Linear and angular velocities were limited up to 0.1 m/s and 0.6 rad/s, respectively. In Fig. 8, some zones are marked in red or grey. A red zone (R1, R2 or R3) indicates when a possible collision is detected, in consequence the robot was stopped (both velocities are null). A grey zone (G1, G2 or G3) indicates

Table II. Results for Destination 2.

		Commands			
Volunteer	Trial	Time [s]	Wrong	Correct	Stop by control system
1	1	166	0	15	0
2	1	159	0	19	0
	1	170	0	18	1
3	2	222	1	27	2
	3	193	0	15	2
4	1	206	2	18	4
5	1	289	3	19	5
6	1	332	11	27	4
	2	232	3	24	0
7	1	363	8	25	5
Average		233.20	2.80	20.70	2.30
Std. Dev.		71.66	3.79	4.64	2.06

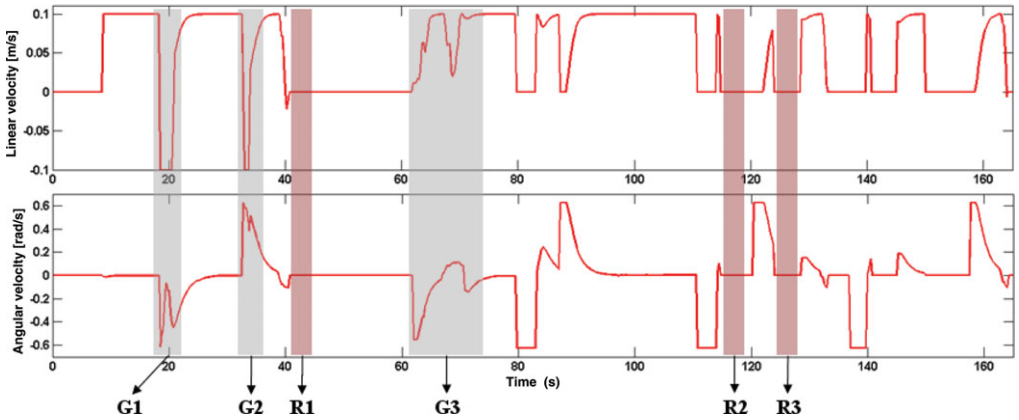

Fig. 8. (Colour online) Robot velocities when Volunteer 5 commanded the robot towards Destination 1. In grey (G1, G2 and G3) an obstacle is evaded and in red (R1, R2 and R3) the robot is automatically stopped to avoid a collision.

when an obstacle is evaded. In G1 the robot turned to the right close to shelves and the control algorithm actuated for avoiding a collision. The same situation was illustrated in G2. Later, the robot approached the doorway (R1), but due to wall proximity and in order to avoid a collision the control system stopped the robot. After that, the system waited for a new command. Afterwards, a new command was conveyed and the robot went through the doorway in G3 and the control system adjusted both velocities in order to avoid hitting the doorway. In R2 the robot performed a turn very close to the desk and in R3 due to the wrong user command, the robot was facing a wall; in both cases the robot was stopped by the control system and it waited for a new command.

A video of the experiment illustrated in these Figures (Volunteer 5 towards Destination 1) is supplied with electronic version of this paper. It shows the path described by the robot, and, simultaneously, the robot velocities and the SSVEP power with its corresponding commands. Another video of Volunteer 3 navigating towards Destination 2 is supplied as well. It shows the path described by the robot, and, simultaneously, the Volunteer 3 operating the system. Here the human–machine interface (with the visual and audible feedback) is observed.

5. Discussion

All the volunteers who participated in this study could navigate the robot towards two different places. The distances from starting point to Destinations 1 and 2 were 7.04 m and 13.9 m, respectively. The average elapsed times for both Destinations were 182 s and 233 s. Comparing Table I versus Table II, volunteers 1 and 2, who attained a higher performance, reached Destination 2 using a lesser number of commands than those used for reaching Destination 1. This is because they felt more confident in

controlling the robot after reaching Destination 1 and they were more familiarized with the system. However, on the average, more commands for Destination 2 (20.7) were required than for Destination 1 (16.9). The average number of wrong commands was similar in both tests (2.13 vs. 2.8). The robot was not stopped by the control system in some trials (volunteers 1, 2 and 6) in Destination 2 (Table II); nevertheless, there was no difference in the average values between both Destinations. Reaching Destination 2 represented a more complicated task, since it was necessary to navigate a corridor, then to pass between two desks and finally turn to the right in order to face the door. The distances among desks (and walls) in Destination 2 were shorter than distances in Destination 1; for instance, desks in Destination 2 were separated by 80 cm and the corridor was 100 cm wide, whereas for Destination 1 desks were separated by 120 cm. However, volunteers did not present any complication in reaching Destination 2, perhaps because they were more familiarized with the system.

Analysis of the results shows that the navigation time with BCI depends not only on the robot velocities and the distance to the destination, but also on other two factors: the performance of each volunteer and the avoidance obstacle algorithm. The first factor is obvious, since higher performance allowed the user to handle more commands to the robot and then, he/she could navigate the robot more precisely. On the other hand, when the robot avoided an obstacle or it adjusted its trajectory to pass through a doorway, the robot reduced its velocities and more time was needed to navigate it, as depicted in Fig. 7.

The control system monitored the distances to any obstacle and, when detected within the rejection area, the robot velocities were modified in order to avoid it. This task needed not an intervention of the user. Should the robot control system not be able to evade the obstacle (say, because it is right in front of the robot or because the obstacle is too close), the system moves the robot 10 cm backward and stops it. Thereafter, the system waits for a new command from the user. In this way, the user maintains almost total control of the robot and only the accurate movements are performed by the control algorithm. Hence, disabled people feel more independent, as they are not supported by a totally automatic system, and so becoming an encouraging situation to carry on with daily life and rehabilitation. Nonetheless, it must be remarked that the robot navigation inside the proposed environment would have been impossible without the control algorithm. Moreover, when the robot was in the corridor and a wrong command was received, the robot rotated and detected the wall, being stopped right off. Without the control algorithm, the robot would hit the wall. We should underline that Figs. 7 and 8 show results obtained from a medium/low-performance user. Volunteers with higher performances accomplished the trial with no errors and, sometimes, the action of the control system was unnecessary (see Table II).

In the proposed scheme, no localization or SLAM systems were used. The desired position (p_2) was estimated based on the commands sent by the user. The goal of the task is to reach Destination 1 or 2 and not the position p_2 itself. Hence, the errors due to odometry are minimal and do not affect the task goal. Moreover, position p_2 is only generated in order to obtain smooth movements since the final and future objective of the current work is that people with disabilities command a robotic wheelchair, where sudden movements must be avoided.

In a previous project,[36] using medium range frequencies (13, 14, 15 and 16 Hz), the subjects express some discomfort with stimuli. In this experiment, using high-frequency range SSVEP no one manifested any complain, furthermore, Volunteer 6 (who participated in both experiments) was delighted with such stimuli. In Prueckl and Guger (2009), three subjects used a BCI to control a mobile robot, when the subject was not looking at the stimuli the robot was stopped.[26] In our work, the robot was still moving in a direction until a new command (a new direction) was indicated. This difference is important since in our approach the subject does not need to gaze at the stimulus every time, only when he/she wants to transmit a command, i.e. our approach is less demanding than in Prueckl and Guger.[26]

The current work has some remarkable points:

(1) Volunteers were not annoyed by the high-frequency flickering of the stimuli;
(2) Volunteers had no previous experience in BCI and they could control the robot swiftly and easily;
(3) Volunteer 2 did not know the environment previous to the experiment, thus this is not a necessary condition to utilize the proposed system;
(4) The environment was not configured for this experiment and the distance among obstacles was just a few centimetres wider than the robot (because of the height of US sensors on robot two

obstacles could not be detected and consequently, they were modified in order to permit the robot detect them).

Escolano *et al.*[16] reported a brain-actuated telepresence system through a mobile robot Pionner 3-DX (the same robot used in the current work), with access to the Internet. The BCI was based on P300 potentials, which were used to select possible target destinations, and then the movement was autonomously executed towards the selected target by the robot. Consequently, both BCI systems used different paradigms; one based on P300, and the other on SSVEP. In our SSVEP-based BCI, the user sent a command with the desired movement (advance, turn left/right or stop) and the robot executed it. Thus, the user exercises more control over the robot movements instead of an automatic movement. To avoid obstacles, Escolano *et al.* equipped the robot with a laser sensor and the navigation system was based on a model builder and a local planner. Herein, the proposed navigation system was simpler; however, more difficult navigation tasks were accomplished. In Escolano *et al.* two navigation tasks were proposed, where the distances among objects were close to 1m or even more. In our work, distances were less than 1m (in some places only a few centimetres longer than the robot dimensions). Besides, the system proposed by Escolano *et al.* had five healthy subjects each with 16 EEG channels. The subjects performed a training phase previously to command the robot. In the current work, only three EEG channels were used and no training phase was needed. This is an important aspect since the user only has to put a few electrodes on his/her head and then he/she is ready to use the system. Finally, in Escolano *et al.*, the robot was controlled in a lab at 260 km through the Internet, while in our case the robot was controlled using Wi-Fi technology (which is limited to approximately 60 m for indoor applications).

Volosyak and colleagues[30] reported on the number of subjects able to use a high-frequency SSVEP-based BCI. They found that only 65.1% of the subjects were able to control a robot with high-frequency SSVEP (34, 36, 38, 40 Hz), in contrast to 97.7% of subjects with medium frequencies (13, 14, 15, 16 Hz). Although, in that paper a robot was commanded by high-frequency SSVEP-based BCI, there are several differences with the current work. First, the focus of both research projects is quite different; in Volosyak *et al.* a statistical study about the number of subjects able to use a high-frequency SSVEP-based BCI, as well as the characteristics of each subject, was performed. While in the current work, a complete strategy in order to control the navigation of a mobile robot is presented, i.e. BCI system and robot control algorithm are presented. Second, in Volosyak *et al.* eight electrodes over the visual cortex for acquiring EEG signals and Minimum Energy Combination method were used. In our work, only three electrodes for EEG acquisition and a simpler method for signal processing were used. This is an important improvement since it is easier and less cumbersome. Third, in Volosyak *et al.* a small (7.5 cm diameter) mobile robot designed for educational purposes (the e-puck[37]) was navigated. In our work, a bigger robot designed for research purposes, the Pioneer 3-DX (44$\times$ 38$\times$ 22 cm) was navigated. Moreover, the robot US sensors were used for avoiding obstacles; for future applications, the robot can carry a payload of up to 23 kg. Fourth, the e-puck was navigated through 25 fixed positions in a small labyrinth, and, thus, the user could see and evaluate the entire scenario where the robot was moved. Moreover, no control algorithm was implemented, since the robot was manually adjusted. In our work, the Pioneer 3-DX was navigated without any fixed positions in a real office-like environment. The user could not see the complete scenario except for the image captured by the camera on the robot, i.e. the robot was remote-commanded. Robot US sensors were used to measure the environment in order to avoid obstacles (or collisions); hence no manual adjustments were necessary since a control algorithm was implemented.

Summarizing, mobile robotic systems commanded by SSVEP-based BCI were reported,[24–26,30] they used more complicated methods for processing EEG and even with more complicated control algorithm based on previous knowledge of the environment. The current work demonstrated that it is possible to control a mobile robot with a SSVEP-based BCI using a simpler method to process EEG and a control algorithm based on fictitious forces to avoid obstacles, without previous knowledge of the environment. Therefore, the current work represents the control of a mobile robot by a high-frequency SSVEP-based self-paced (asynchronous) BCI. High-frequency SSVEP range offers the advantage of a great reduction of visual fatigue caused by flickering[19–22] allowing to use a BCI for longer periods of time. Besides, low and medium frequency SSVEP ranges interfere with alpha rhythm, and could cause an epileptic seizure as well.[23] In related work projects, low and medium frequency ranges were used. In one project stimulation was used up to 16 Hz,[25] in other work the

stimuli were set at 10, 11, 12 and 13 Hz[26] and, finally, it was used from 5 up to 6.9 Hz stimuli.[24] Only one work[30] in related literature (to the best knowledge of these authors) use high-frequency SSVEP for controlling a robot; however, the focus of that work is different, no control algorithm was used and other differences were detailed. Therefore, the present work represents an innovation in the remote control of mobile robotic using a BCI, which is based on high-frequency stimulation.

Finally, the control algorithm and the BCI system can be extended for controlling other mobile vehicles. For example, this BCI system was used for controlling a robotic wheelchair, but neither control system was implemented.[38] The control algorithm presented in this research could easily be transferred to the robotic wheelchair. Consequently, people with disabilities could safely command a robotic wheelchair because the control algorithm prevents collisions. Moreover, they could command it without (or less) visual fatigue due to high-frequency stimulation.

6. Conclusions

This work reports a human–machine interface based on a high-frequency SSVEP-based self-paced (asynchronous) BCI that allows the remote mobile robot navigation in real indoor environments. The BCI system is based on a simple and low computational cost method to classify SSVEP along with a control system to avoid obstacles without previous knowledge of the environment.

All volunteers were able to navigate the mobile robot, independently of their level of expertise in BCI, demonstrating the feasibility of the proposed system. The user visual fatigue was reduced because the user gazed at the stimulus only when a command must be sent to the robot. Furthermore, high-frequency stimulation reduced visual fatigue as well.

The proposed system could be extended for controlling other mobile devices, like a robotic wheelchair. This will represent a useful advantage for people with disabilities, such as quadriplegia. Furthermore, the control system was designed so as to allow disabled people to move about without restrictions because they had full robot movement's control instead of totally automatic systems, encouraging them to continue with daily life and rehabilitation more independently.

Acknowledgements

Authors Diez, Mut and Laciar are supported by Consejo Nacional de Investigación Científica y Tecnológica, CONICET (National Council for Scientific and Technological Research). The authors thank the volunteers for participating in these experiments. Special thanks to Dr. Lucio Salinas and Dr. Victor Andaluz for their invaluable collaboration with the Pioneer robot and to Prof. Dr. Max Valentinuzzi and Prof. Alberto Garcia for grammar reviewing of this paper. Finally, we appreciate the reviewers' suggestions, which improved the quality of this paper.

References

1. S. Mason, J. Kronegg, J. Huggins, M. Fatourechi and A. Schlögl, "Evaluating the Performance of Self-Paced Brain Computer Interface Technology," *Technical Report* (2006). Available at: http://www.bci-info.tugraz.at/Research_Info/documents/articles (accessed March, 2011).
2. R. Scherer, F. Lee, A. Schlögl, R. Leeb, H. Bischof and G. Pfurtscheller, "Toward self-paced brain–computer communication: Navigation through virtual worlds," *IEEE Trans. Biomed. Eng.* **55**(2), 675–682 (2008).
3. J. del R. Millán, F. Renkens, J. Mouriño and W. Gerstner, "Noninvasive brain-actuated control of a mobile robot by human EEG," *IEEE Trans. Biomed. Eng.* **51**(6), 1026–1033 (2004).
4. T. Geng, M. Dyson, C. S. L. Tsui and J. Q. Gan, "A 3-Class Asynchronous BCI Controlling a Simulated Mobile Robot," *Proceedings of the 29th Annual International Conference of the IEEE EMBS*, Lyon, France (Aug. 22–26, 2007) pp. 2524–2527.
5. J. D. Bayliss and D. H. Ballard, "Single trial P3 epoch recognition in a virtual environment," *Neurocomputing* 32–33, 637–642 (2000).
6. V. Hinic, E. M. Petriul and T. E. Whalen, "Human-Computer Symbiotic Cooperation in Robot-Sensor Networks," *Proceedings of Instrumentation and Measurement Technology Conference (IMTC'07)*, Warsaw, Poland (May 1–3, 2007) pp. 1–6.
7. R. Leeb, D. Friedman, G. R. Muller-Putz, R. Scherer, M. Slater and G. Pfurtscheller, "Self-paced (asynchronous) BCI control of a wheelchair in virtual environments: A case study with a tetraplegic," *Comput. Intell. Neurosci.* Article ID 79642 (2007).
8. F. Galan, F. Nuttin, E. Lew, P. W. Ferrez, G. Vanacker, J. Philips and J. del R. Millán, "A brain-actuated wheelchair: Asynchronous and non-invasive brain–computer interfaces for continuous control of robots," *Clin. Neurophysiol.* **119**, 2159–2169 (2008).

9. J. del R. Millán, F. Galan, D. Vanhooydonck, E. Lew, J. Philips and M. Nuttin, "Asynchronous non-invasive brain-actuated control of an intelligent wheelchair" *Proceedings of 31st Annual International Conference of the IEEE EMBS*, Minneapolis, MN, USA (Sep. 3–6, 2009) pp. 3361–3364.
10. A. C. Lopes, U. Nunes, L. Vaz, "Assisted Navigation Based on Shared-Control Using Discrete and Sparse Human-Machine Interfaces," *Proceedings of 32nd Annual International Conference of the IEEE EMBS*, Buenos Aires, Argentina (Aug. 31–Sep. 4, 2010) pp. 471–474.
11. C. J. Bell, P. Shenoy, R. Chalodhorn and R. P. N. Rao, "Control of a humanoid robot by a noninvasive brain–computer interface in humans," *J. Neural Eng.* **5**, 214–220 (2008).
12. R. Scherer, M. Chung, J. Lyon, W. Cheung and R. P. N. Rao, "Interaction with Virtual and Augmented Reality Environments Using Non-Invasive Brain-Computer Interfacing," *Proceedings of ICABB*, Venice, Italy (Oct. 14–16, 2010).
13. R. Ron-Angevin, F. Velasco-Alvarez, S. Sancha-Ros and L. da Silva-Sauer, "A Two-Class Self-Paced BCI to Control a Robot in Four Directions," *Proceedings of IEEE International Conference on Rehabilitation Robotics Rehab*, Zurich, Switzerland (Jun. 29–Jul. 1, 2011) pp. 1–6.
14. I. Iturrate, J. Antelis, J. Minguez and A. Kübler, "A non-invasive brain-actuated wheelchair based on a P300 neurophysiological protocol and automated navigation," *IEEE Trans. Robot*. **25**(3), 614–627 (2009).
15. C. Escolano and J. Minguez, "Sistema de teleoperación multi-robot basado en interfaz cerebro-computador," *Revista Iberoamericana de Automática e Informática Industrial (RIAII)* **8**(2), 16–23 (2011).
16. C. Escolano, J. M. Antelis and J. Minguez, "A telepresence mobile robot controlled with a noninvasive brain–computer interface," *IEEE Trans. Syst. Man Cybern.* **42**(3), 793–804 (2012).
17. D. Regan, *Human Brain Electrophysiology: Evoked Potentials and Evoked Magnetic Fields in Science and Medicine* (Elsevier, New York, 1989).
18. C. S. Herrmann, "Human EEG responses to 1–100 Hz flicker: Resonance phenomena in visual cortex and their potential correlation to cognitive phenomena," *Exp. Brain. Res*. **137**, 346–353 (2001).
19. Y. Wang, R. Wang, X. Gao, B. Hong and S. Gao, "A practical VEP-based brain–computer interface," *IEEE Trans. Neural Syst. Rehab. Eng.* **14**(2), 234–239 (2006).
20. G. Garcia Molina and V. Mihajlovic, "Spatial filters to detect steady-state visual evoked potentials elicited by high frequency stimulation: BCI application," *Biomed. Tech.* **55**, 173–182 (2010).
21. A. Materka, M. Byczuk and P. Poryzala, "A Virtual Keypad Based on Alternate Half-Field Stimulated Visual Evoked Potentials," *Proceedings of International Symposium on Information Technology Convergence*, Joenju, South Korea (Nov. 23–24, 2007) pp. 296–300.
22. Y. Wang, R. Wang, X. Gao and S. Gao, "Brain-Computer Interface Based on the High-Frequency Steady-State Visual Evoked Potential," *Proceedings of 1st International Conference on Neural Interface and Control*, Wuhan, China (May 26–28, 2005) pp. 37–39.
23. R. S. Fisher, G. Harding, G. Erba, G. L. Barkley and A. Wilkins, "Photic and pattern induced seizures: A review for the Epilepsy Foundation of America Working Group," *Epilepsia* **46**(9), 1426–1441 (2005).
24. S. M. Torres Müller, T. Freire Bastos-Filho, W. Cardoso Celeste and M. Sarcinelli-Filho, "Brain-computer interface based on visual evoked potentials to command autonomous robotic wheelchair," *J. Med. Biol. Eng.* **30**(6), 407–416 (2010).
25. C. Mandel, T. Lüth, T. Laue, T. Röfer, A. Gräser and B. Krieg-Brückner, "Navigating a Smart Wheelchair with a Brain-Computer Interface Interpreting Steady-State Visual Evoked Potentials," *Proceedings of IEEE/RSJ International Conference on Intelligent Robots and Systems*, St. Louis, MO, USA (Oct. 10–15, 2009) pp. 1118–1125.
26. R. Prueckl and C. Guger, "A Brain–Computer Interface Based on Steady State Visual Evoked Potentials for Controlling a Robot," *Proceedings of the 10th International Work-Conference on Artificial Neural Networks (IWANN '09)*, Salamanca, Spain (Jun. 10–12, 2009).
27. G. R. Müller-Putz and G. Pfurtscheller, "Control of an electrical prosthesis with an SSVEP-based BCI," *IEEE Trans. Biomed. Eng*. **55**(1), 361–364 (2008).
28. S. M. Grigorescu, T. Lüth, C. Fragkopoulos, M. Cyriacks and A. Gräser, "A BCI controlled robotic assistant for quadriplegic people in domestic and professional life," *Robotica* **30**(3), 419–431 (2012). doi:10.1017/S0263574711000737.
29. P. F. Diez, V. A. Mut, E. Avila Perona and E. Laciar Leber, "Asynchronous BCI control using high-frequency SSVEP," *J. Neuro. Eng. Rehab.* **8**(39), 1–8 (2011).
30. I. Volosyak, D. Valbuena, T. Lüth, T. Malechka and A. Gräser, "BCI demographics II: How many (and what kinds of) people can use a high-frequency SSVEP BCI?" *IEEE Trans. Neural Syst. Rehab. Eng.* **19**(3), 232–239 (2011).
31. R. Carelli, H. Secchi and V. Mut, "Algorithms for stable control of mobile robots with obstacle avoidance," *Latin Am. Appl. Res.* **29**(3), 191–196 (1999).
32. H. Secchi, R. Carelli and V. Mut, "Discrete Stable Control of Mobile Robots with Obstacle Avoidance," *Proceedings of the International Conference on Advanced Robotics (ICAR'01)*, Budapest, Hungary (Aug. 22, 2001) pp. 405–441.
33. V. Mut, R. Carelli and B. Kuchen, "Adaptive impedance control for robot with sensorial feedback (in Spanish)," *Proceedings of XIII National Symposium of Automatic Control (AADECA)*, Buenos Aires, Argentina (Oct. 1992) pp. 345–349.
34. J. Borenstein and Y. Koren, "The vector field histogram-fast obstacle avoidance for mobile robots," *IEEE Trans. Robot. Autom*. **7**(3), 278–288 (1991).

35. R. Carelli and E. Oliveira Freire, "Corridor navigation and wall-following stable control for SONAR-based mobile robots," *Robot. Auton. Syst.* **45**, 235–247 (2003).
36. P. F. Diez, V. Mut, E. Laciar and E. Avila, "A Comparison of Monopolar and Bipolar EEG Recordings for SSVEP Detection," *Proceedings of 32nd Annual International Conference of the IEEE EMBS*, Buenos Aires, Argentina (Aug. 31–Sep. 4, 2010) pp. 5803–5806.
37. F. Mondada, M. Bonani, X. Raemy, J. Pugh, C. Cianci, A. Klaptocz, S. Magnenat, J. Zufferey, D. Floreano and A. Martinoli, "The e-Puck, A Robot Designed for Education in Engineering," *Proceedings of the 9th Conference on Autonomous Robot Systems and Competitions*, Castelo Branco, Portugal (May 7, 2009) pp. 59–65.
38. P. F. Diez, S. M. Torres Müller, V. A. Mut, E. Laciar, E. Avila, T. Freire Bastos-Filho and M. Sarcinelli-Filho, "Commanding a robotic wheelchair with a high-frequency steady-state visual evoked potential based brain–computer interface," *Med. Eng. Phys.* **35**(8), 1155–1164 (2013). Available at: http://dx.doi.org/10.1016/j.medengphy.2012.12.005